

Supporting Information

Facile one-pot nanoproteomics for label-free proteome profiling of 50-1000 mammalian cells

Kendall Martin^{1,2#}, Tong Zhang^{1#}, Tai-Tu Lin¹, Amber N. Habowski³, Rui Zhao⁴, Chia-Feng Tsai¹, William B. Chrisler¹, Ryan L. Sontag¹, Daniel J. Orton¹, Yong-Jie Lu⁵, Karin D. Rodland¹, Bin Yang^{1,2}, Tao Liu¹, Richard D. Smith¹, Wei-Jun Qian¹, Marian L. Waterman³, H. Steven Wiley⁴, Tujin Shi^{1*}

¹Biological Sciences Division, Pacific Northwest National Laboratory, Richland, Washington 99354, USA.

²Bioproducts, Sciences & Engineering Laboratory, Department of Biological Systems Engineering, Washington State University, Richland, WA 99354, USA.

³Department of Microbiology and Molecular Genetics, University of California Irvine, Irvine, California 92697, USA.

⁴Environmental Molecular Sciences Laboratory, Pacific Northwest National Laboratory, Richland, Washington 99354, USA.

⁵Centre for Cancer Biomarker and Biotherapeutics, Barts Cancer Institute, Queen Mary University of London, London EC1M 6BQ, United Kingdom.

#K.M. and T.Z. contributed equally to this manuscript.

***Corresponding author:**

Dr. Tujin Shi
Integrative Omics Group
Biological Sciences Division
Pacific Northwest National Laboratory
Richland, WA 99352
Tel: (509)371-6579
Email: tujin.shi@pnnl.gov

Supplemental Figure 1. The peptide/proteome coverage at different processing volumes by two different searching software tools.

Supplemental Figure 2. Boosting effects of “the match between runs (MBR)” on peptide and protein identification.

Supplemental Figure 3. Venn diagrams showing the number of protein groups identified from each of 3 biological replicates at different numbers of cells.

Supplemental Figure 4. Pairwise correlation of protein LFQ intensities between any two replicates for different numbers of cells.

Supplemental Figure 5. Schematic diagram for dissociation of mouse colon tissues, the locations of five crypt cell subpopulations, and their isolation by FACS.

Supplemental Figure 6. Volcano plots showing the proteome differences among different colon crypt cell types.

Supplemental Table 1. Protein identification and LFQ quantification in 50-1000 MCF10A cells using SOPs-MS.

Supplemental Table 2. Protein identification and LFQ quantification in colon crypt cell types using SOPs-MS.

Supplemental Table 3. Comparison of SOPs-MS with existing nanoproteomics approaches for analysis of small number of cells.

Supplemental Figure 1

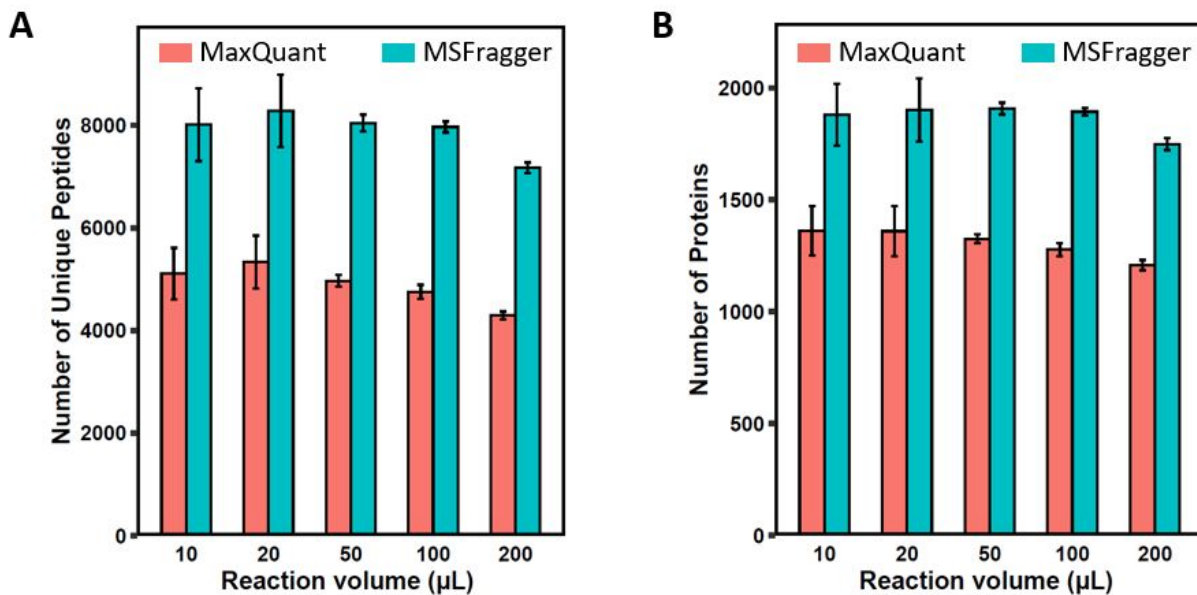


Figure S1. The peptide/proteome coverage by two different searching software tools. **(A)** The number of identified unique peptides using MaxQuant and MSFragger. **(B)** The number of identified protein groups using MaxQuant and MSFragger. Red bar: MaxQuant; blue bar: MSFragger. Data are shown as the mean value \pm SD. Note that the actual MS/MS spectra were used for searching and that the same parameters including the false discovery rate (FDR) at both the peptide and protein levels were used.

Supplemental Figure 2

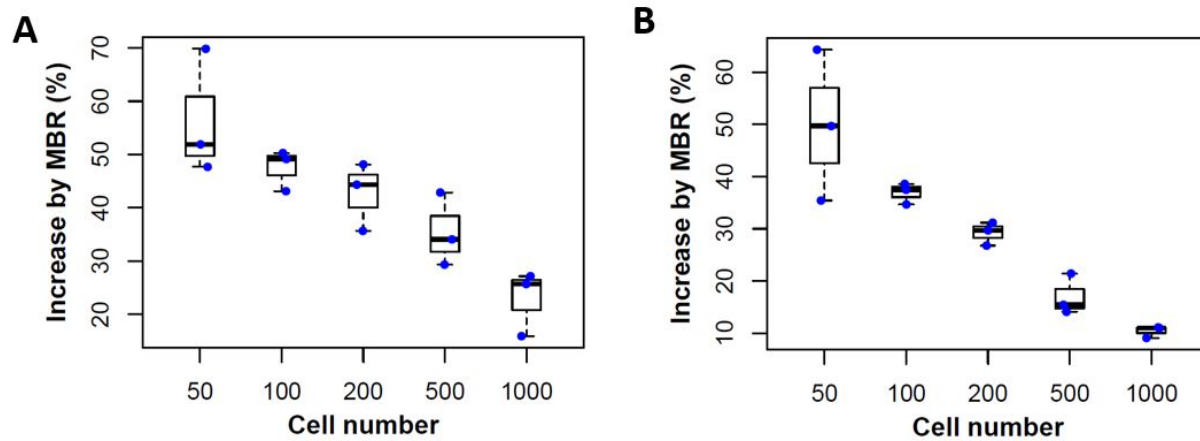


Figure S2. Boosting effects of “the match between runs (MBR)” on peptide and protein identification. The percentage increased by MBR for the number of peptides (**A**) and protein groups (**B**) was plotted as a function of the number of cells.

Supplemental Figure 3

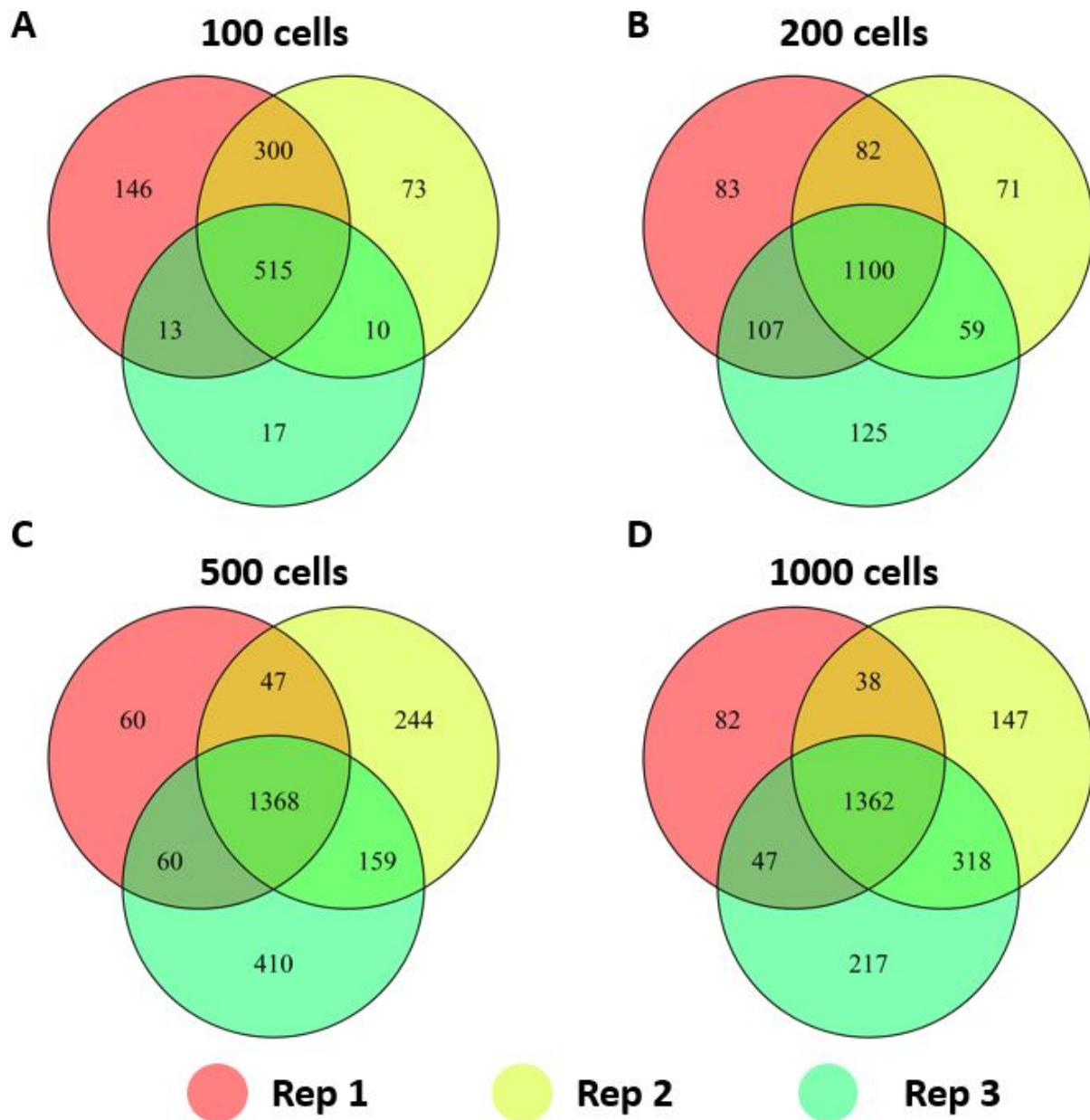


Figure S3. Venn diagrams showing the number of protein groups identified from each of 3 biological replicates for (A) 100 MCF10A cells, (B) 200 MCF10A cells, (C) 500 MCF10A cells, and (D) 1000 MCF10A cells.

Supplemental Figure 4

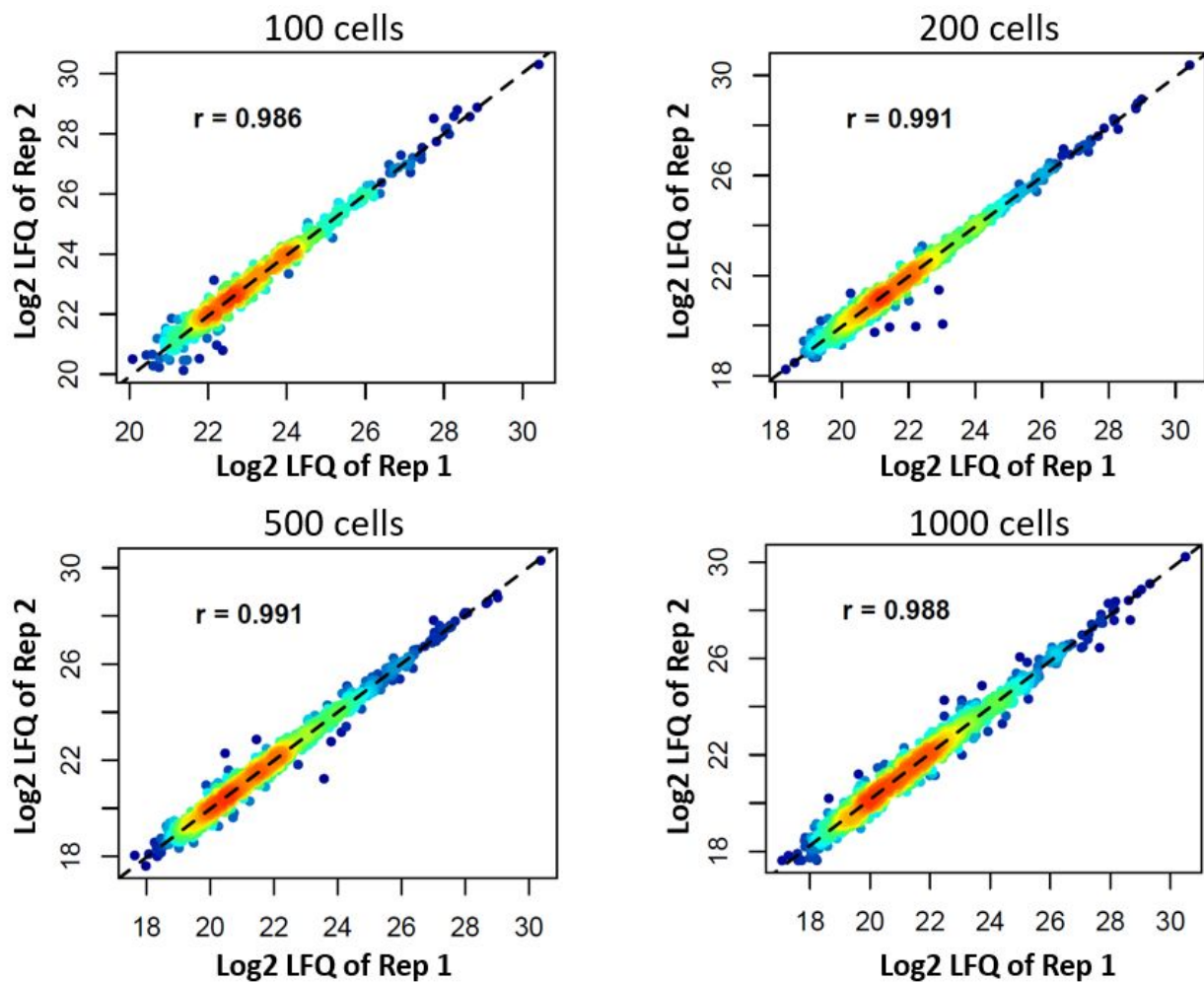
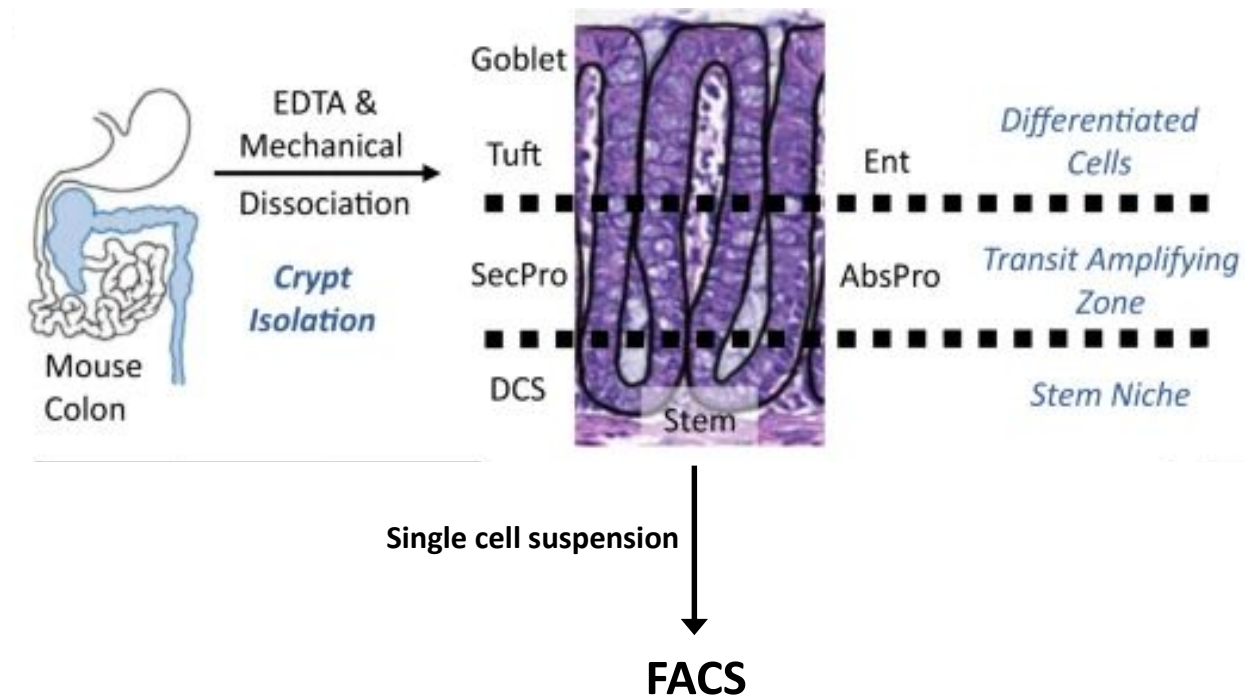


Figure S4. Pairwise correlation of protein LFQ intensities between any two replicates for 100, 200, 500, and 1000 MCF10A cells with the Pearson correlation coefficients. Color scale indicates the density of the data point (low to high in blue to red).

Supplemental Figure 5



Tube#	Mouse#	Sample type	Cell Type	Cell#	Avg#
1	1	BR1	Stem	1299	1490
2	1	BR1	SecPDG	247	480
3	1	BR1	AbsPro	1482	1691
4	1	BR1	Tuft	138	141
5	1	BR1	ENT	1037	1563
6	2	BR2	Stem	2036	
7	2	BR2	SecPDG	482	
8	2	BR2	AbsPro	1557	
9	2	BR2	Tuft	148	
10	2	BR2	ENT	1673	
11	3	BR3	Stem	1136	
12	3	BR3	SecPDG	710	
13	3	BR3	AbsPro	2035	
14	3	BR3	Tuft	136	
15	3	BR3	ENT	1980	

Figure S5. Schematic diagram for dissociation of mouse colon tissues, the locations of five crypt cell subpopulations, and their isolation by FACS. The table listed the number of FACS-sorted cells for each subpopulation of mouse colon crypt cells.

Supplemental Figure 6

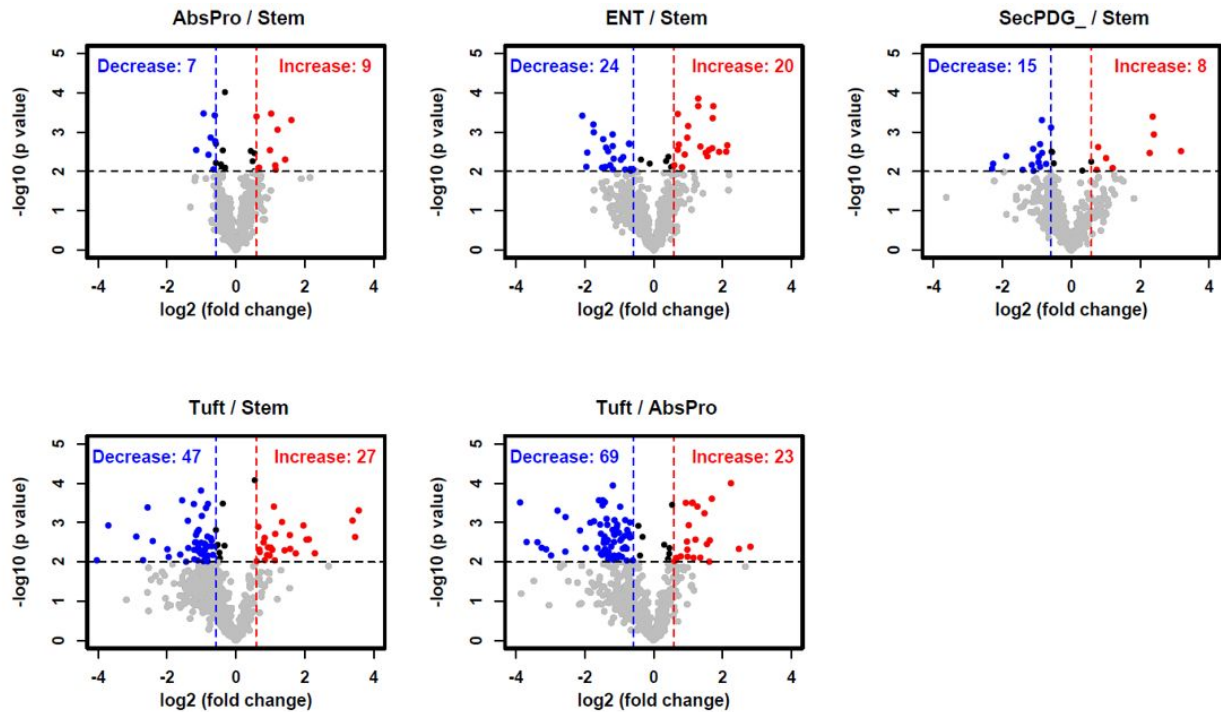


Figure S6. Volcano plots showing the proteome differences among different colon crypt cell types. Horizontal dashed black line: p value = 0.01 as one cutoff to define statistical significance. Vertical dashed bed and red line: fold change of 50% as another cutoff to define significantly differential proteins.

Supplemental Table 1. Protein identification and LFQ quantification in 50-1000 MCF10A cells using SOPs-MS.

See [Table S1.xlsx](#) for details.

Supplemental Table 2. Protein identification and LFQ quantification in colon crypt cell types using SOPs-MS.

See [Table S2.xlsx](#) for details.

Supplemental Table 3. Comparison of SOPs-MS with existing nanoproteomics approaches for analysis of small number of cells.

See [Table S3.xlsx](#) for details.